Single-electron tunnelling in few-atom systems: size of single atoms and geometry of few-atom clusters

2001 J. Phys.: Condens. Matter 13 1819

(http://iopscience.iop.org/0953-8984/13/9/305)

INSTITUTE OF PHYSICS PUBLISHING JOURNAL OF PHYSICS: CONDENSED MATTER

J. Phys.: Condens. Matter **13** (2001) 1819–1826 www.iop.org/Journals/cm PII: S0953-8984(01)15497-4

Single-electron tunnelling in few-atom systems: size of single atoms and geometry of few-atom clusters

S T Ruggiero and T B Ekkens

Department of Physics, University of Notre Dame, Notre Dame, IN 46556, USA

E-mail: ruggiero.1@nd.edu

Received 14 July 2000, in final form 21 November 2000

Abstract

We show results for tunnelling into single atoms and few-atom clusters. Single-electron tunnelling with STM reveals a clear series of cluster capacitance in a 2:3:4 ratio corresponding to single atoms or dimers, three-atom clusters and four-atom clusters. We present results for Ag and Bi atoms, which have similar nearest-neighbour distances but are otherwise dissimilar. Qualitatively, we conclude that tunnelling electrons occupy anti-bonding-like configurations on the clusters. Quantitatively our results imply an atomic diameter—or few-atom cluster bond length—of 2.6 ± 0.1 Å for these species.

1. Introduction

Studies of small clusters of metals and other materials are a topic of wide ranging importance. Clusters are of interest from the standpoint of chemical reaction kinetics and new material systems such as the fullerenes and vapour-deposited biomolecules [1]. They serve as model systems for the study of surfaces and interfaces, and are key to understanding the evolution from single atom properties to those of bulk materials [2]. Their geometry, spectroscopy, chemistry and material and electronic properties, especially as compared to the bulk, are the subject of broad interest. Part of the recent success of such studies lies in new tools now available to study even the smallest physical systems, down to single atoms. In this paper we describe the results of single-electron tunnelling (SET) into single- and few-atom clusters of Ag and Bi using scanning tunnelling microscopy (STM). We show for the first time that spectroscopic tunnelling measurements of few-atom clusters can accurately determine atomic sizes, details of the free-electron density in clusters and the geometrical progression of cluster types. We note that this approach to cluster study is easily open to the many systems which can be prepared as small clusters on surfaces.

STM has proven to be a tool with considerable value beyond its original role of surface imaging. Employed spectroscopically, STM can probe the local tunnelling density of states and as such has been used in revealing studies of high-temperature superconductors and other layered systems [3]. If tunnelling occurs into a sufficiently small object deposited on a thin dielectric barrier, single-electron tunnelling (SET) can also be observed with STM. Since the

0953-8984/01/091819+08$30.00

object is not maintained at the Fermi level of either electrode, its capacitance (size and geometry) can be revealed by SET. These effects are clearly evident in metal droplets [4] down to the atomic scale [5]. As succinctly noted by Apell and Tagliacozzo [6] any extra energy associated with image charges, work functions, etc is always in balance for incoming and outgoing electrons and is not manifest in the resulting current–voltage characteristics. We can even rule out double charging because of the so-called 'Coulomb explosion' in small droplets [7]. Added to charging effects can be elements of the intrinsic tunnelling density of states of the object including quantum size effects, etc. However, the dominant feature for SET is a staircase-like current–voltage characteristic with voltage steps of width e/C, where e is the electronic charge and C is the capacitance of the object being tunnelled into.

For our studies we chose Ag and Bi since they both readily form ultra-small droplets and have closely matched lattice constants in the bulk, but have dissimilar chemical and Fermi properties. For monolayer depositions of these materials our results reveal a clear distribution of single-electron step widths (equal for Ag and Bi clusters, as expected) that corresponds to tunnelling into objects with capacitances in the ratio of 2:3:4. We show that this naturally corresponds to single atoms or dimers, three-atom clusters and four-atom clusters, respectively. This correspondence is based on a simple model where each new atom introduced into a cluster adds an additional capacitance equal to half of that for a single atom. The absolute size and shape of these clusters deduced from this model are in good accord with theoretical and experimental results for Ag dimer systems.

2. Experiment

This work was performed with a standard design [3] low-temperature STM, with the sample and all working elements of the microscope in contact with liquid cryogens. The design incorporated lead zirconate titanate ceramic (PZT) piezo-electric elements suitable for operation at both 77 and 4.2 K, the latter used in these experiments, and typical data for which are shown in figure 1. Tunnelling tips were produced by clipping the end of a 0.06 inch diameter Pt/Ir alloy (80/20) wire, and a newly produced tip was used for each run of the microscope.

Samples were prepared by thermal evaporation onto polished electronic-grade [110] Si wafers. Evaporations were performed in a diffusion-pumped high-vacuum system with a base pressure of 1×10^{-8} Torr. For a given sample, a 1500 Å layer of Al was first deposited to form a base electrode, which was briefly exposed to air to form a (10–15 Å thick) Al_2O_3 tunnel barrier. Next, a thin ($<$100 Å) layer of Ag or Bi was deposited on the Al_2O_3 surface to produce a layer of droplets, completing the simple process of sample preparation. Tungsten thermal evaporation 'boats' were used for Al evaporations. The boat was heated to the melting point of Al (660 °C) and the power adjusted to achieve a deposition rate of $\sim$20 Å s^{-1}, after which a layer of the desired thickness (1500 Å) was deposited. For the preparation of droplet layers, films of Bi (melting point 271 °C) and Ag (melting point 961 °C) were similarly deposited from Ta or Mo boats at rates of $\leqslant$5 Å s^{-1}.

This technique of producing a layer of ultra-small metal droplets is based on the well known fact that films of metals including Ag, Au, Cu, In, Pb, Sn etc less than roughly 100 Å in thickness tend to form isolated droplets rather than a continuous layer [8–10]. This is also true for Bi [11], which can be prepared with a maximum droplet size of roughly 80 Å. For comparative purposes, and mindful that Bi is particularly subject to oxidation, measurements on all samples were made repeatedly over a period of roughly three days after which steps could typically no longer be seen.

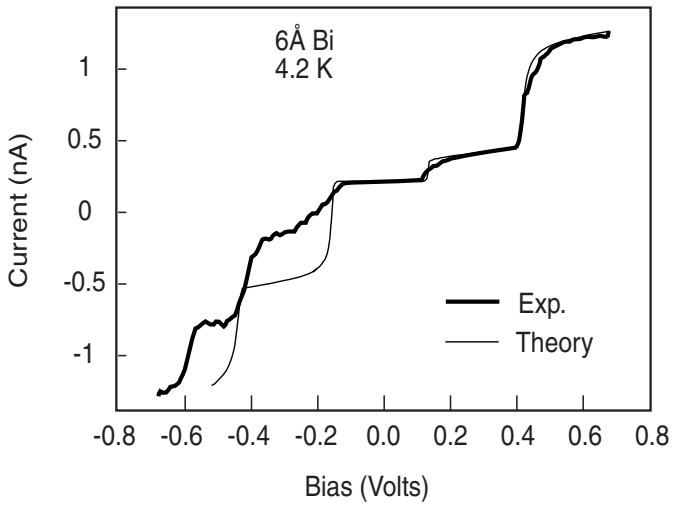

Figure 1. Shown is an STM current–voltage trace of a 6.0 Å diameter Bi droplet exhibiting single-electron steps. Also included is a $T = 4.2$ K fit to the data with the semi-classical single-electron tunnelling theory [12]. Parameters for this sample are $C = 5.6 \times 10^{-19}$ F and $R = 376$ MΩ.

3. Results and discussion

Tunnelling into an isolated object with capacitance C will produce a current–voltage curve characterized by a series of steps of width $\Delta V = e/C$, where e is the electron charge. This series of steps comprises a single-electron 'Coulomb staircase' [12]. An isolated sphere of diameter d embedded in an infinite dielectric medium of constant κ has a capacitance $C = 2\pi\kappa\varepsilon_0 d$, where $\varepsilon_0 = 8.854 \times 10^{-12}$ F m^{-1}. Therefore, the single-electron step width will be given as

$$\Delta V = \frac{e}{2\pi\kappa\varepsilon_0 d} = \frac{28.8}{\kappa d} \tag{1}$$

where ΔV is in volts and d is in Å.

In the case of STM, the tip is brought into tunnelling range of a droplet and the tunnel current is measured as a function of the tip bias with respect the base electrode. Because of the thin (10–15 Å) Al_2O_3 film between the base electrode and a cluster, and the proximity of the base electrode and tip, geometrical as well as dielectric effects can contribute to the apparent droplet capacitance.

A sample tunnelling characteristic for a 6 Å Bi droplet is shown in figure 1. Clearly evident is the expected Coulomb staircase. We note that the tip position was adjusted to produce current–voltage characteristics with optimized gap structure (low-dynamic-resistance regions on the Coulomb staircase). Tunnelling into oxidized continuous films of Al and Bi, where no isolated droplets were present, shows no Coulomb staircase behaviour under any circumstances [13]. Also shown is the result for the semi-classical single-electron tunnel theory [14, 15], which is in good general accord with the data. We note that certainly higher levels of symmetry and adherence to theory are achievable with STM. For example, by using relatively large (∼100 Å) Sn droplets [4]. Nonetheless, the degree of compliance with theory achieved with the systems studied here allows for the unambiguous determination of the Coulomb step width—well within the uncertainty represented by the size of all plotted data points.

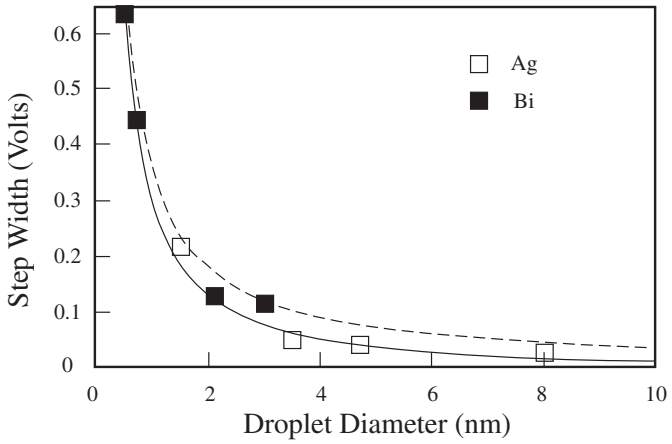

Figure 2. Plotted is the single-electron step width, ΔV, as a function of droplet diameter. The solid line is the theoretical result for an isolated sphere in an infinite dielectric medium (equation (1)) and the dotted curve the same result modified to include the geometrical effects of the tunnelling electrodes (equation (2)).

In sandwich junction experiments with Ag, Cu, Pb and Sn, where there is both a top and bottom electrode and tunnelling takes place into many droplets, it has been shown [16] that step width correlates well with a simple model which includes the effects of geometrical capacitance by adopting a simple spherical capacitor model. The model assumes that a spherical droplet is completely surrounded by a uniform layer of oxide of thickness s in turn covered by a conducting shell. This results in the expression

$$\Delta V = \frac{28.8}{\kappa d}\left(\frac{2s}{2s+d}\right) \tag{2}$$

where again d is the droplet radius in Å, ΔV is the step width in volts and here s is the oxide thickness in Å. Thus equations (1) and (2) represent respectively the two extreme possibilities: a completely isolated droplet in an infinite dielectric medium and a droplet surrounded by the same dielectric which is in turn surrounded by a concentric metal shell.

In figure 2 we show the single-electron step width, ΔV, versus inverse droplet diameter for Ag and Bi. Each point represents an average of all the data taken at a given deposited thickness. To fit the data in this size regime we show both the isolated sphere model, from equation (1) (solid line) and the concentric sphere model, equation (2) (dashed line). In the latter case a value of $s = 25$ Å was used although values of 10 to 30 Å provide similar fits. We see that the data lie, as expected, between these two extremes although both models follow the data well. Here we have taken $\kappa = 9.5$, which compares well with values of 8 [17]–9.3 [18] for Al_2O_3 and noting that for Bi_2O_3 $\kappa = 18.2$ [18]. Note that for Bi and Pb the data are averaged over various stages of oxidation. Thus in this size regime at least the measured step width seems always to correspond exclusively to the deposited droplet size.

This result is corroborated by previous studies where Ag and Pb droplets were directly imaged with STEM (scanning transmission electron microscopy) and it was found that the average droplet diameter was indeed equal to the nominal deposited film thickness and that the measured distribution of droplet diameters corresponds exactly to the distribution of single electron step widths [16]. Similar results were also found for In droplets [10]. Thus the correlation of measured step width to droplet size (and deposited film thickness) for relatively large droplets has been well established.

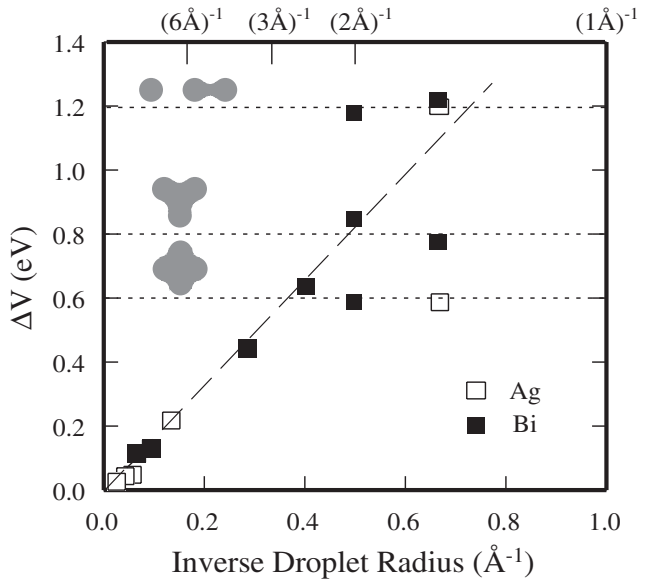

Figure 3. Shown is the single-electron step width ΔV as a function of inverse droplet radius. For average radii below 6 Å, the data break up into distinct bands. Above 6 Å (data on the left side of the plot), ΔV is a continuous function of inverse particle size. Shown is a progression of cluster geometries consistent with the observed series of discrete step-width levels. The atomic diameter associated with the top-most level (twice the intercept value shown on the plot) is 2.6 ± 0.1 Å.

The goal of the present work was to explore the regime where the idea of an average droplet diameter breaks down—to where it is more appropriate to view the systems as clusters of one, two or a few atoms. This is achieved by depositing monolayer and sub-monolayer films. In this regime we have focused on Bi and Ag to compare systems with very different bulk Fermi properties but with similar structural parameters. Also, Ag is an otherwise well studied cluster system.

In figure 3 we show data down to sub-monolayers of deposited material. Larger size droplets clearly conform well to the expected $1/r$ behaviour. However, as the deposited thickness drops to the vicinity of a monolayer, the observed step widths clearly break up into discrete levels—independent of deposited thickness. This phenomenon is also clearly manifest in figure 4, which shows the distribution of step widths for all data below 6 Å. Peaks with mean values of 0.59, 0.81 and 1.2 eV are clear. We note that the number of data points plotted is a reflection of the relatively few clusters in this size range which produced single-electron step behaviour with similar characteristics to those shown in figure 1. Samples produced by depositions in the very lowest thickness regimes always exhibited far fewer 'active' tunnel sites than those produced at larger deposition thickness.

Based on the results for larger-diameter clusters, 1.2 eV would correspond to a 2.52 Å diameter droplet based on the isolated-sphere model and a 2.66 Å diameter droplet based on the spherical capacitor model. Thus, it is fair to conclude from our data that the effective diameter of a single atom is 2.6 ± 0.1 Å. We return to the issue of cluster size and type below.

If we take C_a as the value of the capacitance assigned to a single atom (with an associated charging energy of $\Delta V = 1.2$ eV) then, with $C = e/\Delta V$, the capacitances associated with steps at charging energies of 1.2, 0.8 and 0.6 eV will correspond to values of capacitance of C_a, $\frac{3}{2}C_a$ and $2C_a$, respectively. That is, this sequence of charging energies has associated with it

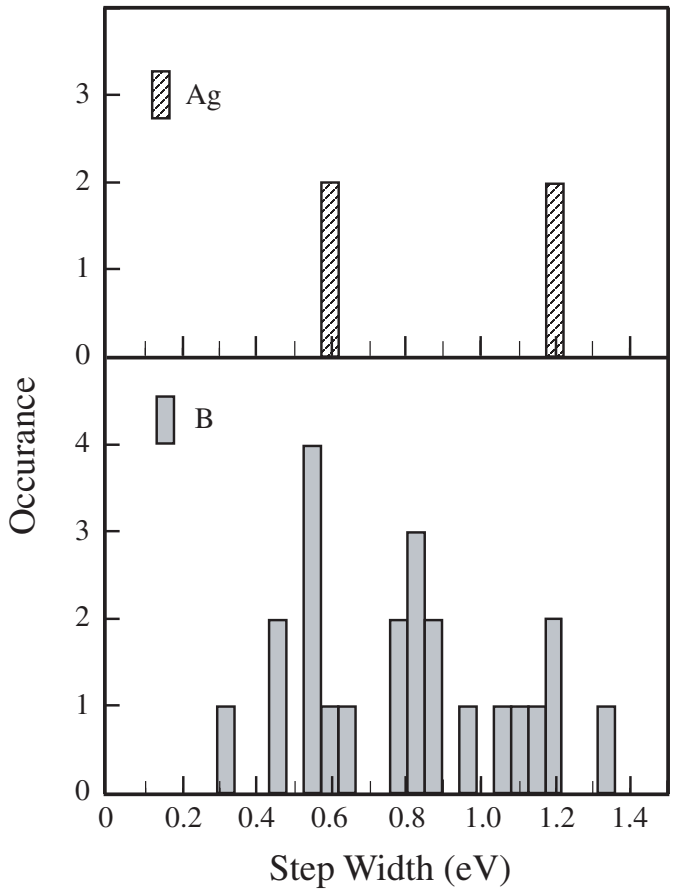

Figure 4. Shown is the distribution of step widths recorded for the smallest size clusters shown separately for Ag and Bi. Clear are peaks in the step width, which occur at mean values of 0.59, 0.81 and 1.2 V.

the presence of objects which have capacitances in a 2:3:4 ratio. In addition, it appears that the 1.2 eV step is associated with clusters of both one and two atoms, the 0.8 eV peak with three atoms and the 0.6 eV peak with four-atom clusters. That the first level is 'degenerate' with respect to geometry is consistent with the simple model that a tunnelling electron occupies an anti-bonding-like state with its charge density localized at regions of positive curvature of the neutral clusters. For Ag_2^- the added electron density of a tunnelling electron would thus occupy hemispherical caps on the ends of the formerly neutral cluster which has a 'peanut-like' shape. This qualitative picture is consistent with charge density calculations for the bonding and anti-bonding states of Ag_2 [19] (which exhibits a predominant s-wave character) and the macroscopic paradigm where free charge resides on the convex surfaces of a conducting object. Thus the capacitance of a dimer (Ag–Ag) or (Bi–Bi) will be the same as that for two halves of a single atom. So each atom in a two-atom cluster contributes half the capacitance of a single atom for a total of C_a, each atom in a three-atom cluster contributes half the capacitance of a single atom for a total of $\frac{3}{2}C_a$ and so on. Thus for two-, three- and four-atom clusters we get a $\frac{2}{2}:\frac{3}{2}:\frac{4}{2}$ or 2:3:4 ratio of capacitance. This sequence is depicted pictorially in figure 3.

Physical configurations other than those depicted in figure 3 are possible for clusters of three and four atoms. For example, *linear* trimers may well be present [20] as well as extended linear objects comprised of van der Waals coupled chains of dimers [21]. Indeed, as seen in figure 4, a number of objects appear to be present with capacitances off the observed sequence. Nonetheless, the very well defined series of observed capacitances, the absolute magnitude of these capacitances and general STM observations of Ag and other clusters are consistent with the presence of one-/two-atom, three-atom and four-atom clusters as depicted in the figure.

Returning to the issue of absolute atomic size, we note that in the bulk, Ag and Bi have nearest-neighbour distances of 2.89 and 3.07 Å, respectively [22]. However, for large clusters—in the size regime where a number of atomic layers are present—there is an observed interlayer contraction, which in Cu corresponds to an interlayer bond length decrease of roughly 3 to 5% [23]. Likewise, for few-atom clusters comparable contraction is observed. For example, energy-level and electron density calculations of Ag_2 have been made as a function of inter-atomic spacing and compared to measured spectra [19]. For Ag_2 clusters in solid inert-gas matrices and in the gas phase, calculations for Ag–Ag separations of 2.5 and 2.8 Å appear to more closely represent these data, respectively. Other calculations for free Ag_2 and Ag_3 bond lengths have been reported [24] as 2.5 and 2.5–2.6 Å, respectively. Finally, STM imaging of Ag dimers and trimers on graphite [20] gives a Ag–Ag bond length of 2.5 ± 0.2 Å. Thus the value from this work of 2.6 ± 0.1 Å compares well with these results and may suggest that variations in reported values are associated with the Ag_2 environment.

4. Conclusions

In conclusion, we have studied few-atom clusters of Ag and Bi with STM employing single-electron tunnelling. The capacitance of the clusters occurs in a 2:3:4 ratio, suggesting we are viewing one-/two-atom, three-atom and four-atom clusters, respectively. The observed sequence in and absolute magnitude of capacitance implies a progression in cluster geometry whereby each additional atom added to a cluster contributes to it an additional convex surface with the capacitance of half of a single atom. This interpretation is based on a primitive model, wherein a tunnelling electron occupies an anti-bonding-like state with its charge density localized at the regions of positive curvature of the clusters. We have seen that as expected the results are independent of atomic species with similar bulk nearest-neighbour distances (here Ag and Bi). We can also derive the size of the clusters, and our results give an atomic diameter of 2.6 ± 0.1 Å. This is within the range of previous Ag cluster results and may be of sufficient resolution to explore few-atom cluster bond-lengths as a function of substrate.

Acknowledgments

We gratefully acknowledge insightful discussions with G B Arnold and support by the DOE through grant DE FG02 88 ER45373.

References

[1] See Weisendanger R 1994 *Scanning Probe Microscopy and Spectroscopy* (New York: Cambridge)
[2] See, for example, Pacchioni G, Bagus P S and Parmigiani F 1992 *Cluster Models for Surface and Bulk Phenomena* (New York: Plenum)
[3] Stroscio J A and Kaiser W J 1993 *Scanning Tunnelling Microscopy* (New York: Academic)
See Edwards H L, Derro D J, Barr A, Markert J and de Lozanne A 1995 *Phys. Rev. Lett.* **75** 1387 and references therein

[4] Wilkins R, Ben-Jacob E and Jaklevic R C 1989 *Phys. Rev. Lett.* **63** 801
[5] Ralph D C, Blanck C T and Tinkham M 1995 *Phys. Rev. Lett.* **74** 3241
[6] Apell P and Tagliacozzo A 1988 *Phys. Status Solidi* **145** 483
[7] Sattler K, Muehlbach J, Echt O, Pfau P and Recknagel E 1981 *Phys. Rev. Lett.* **47** 160
Iakubov I T, Khrapak A G, Podlubny L I and Pogosov V V 1985 *Solid State Commun.* **53** 427
[8] Pashley D W, Stowell M J, Jacobs M H and Law T J 1964 *Phil. Mag.* **10** 127
[9] van Loen E J, Iwami M, Tromp R M, van der Veen J M and Saris F W 1983 *Thin Solid Films* **104** 9
[10] Lambe J and Jaklevic R C 1969 *Phys. Rev. Lett.* **22** 789
[11] Cohn J L and Uher C 1989 *J. Appl. Phys.* **66** 2045
[12] Mullen K, Ben-Jacob E, Jaklevic R C and Schuss Z 1988 *Phys. Rev.* B **37** 98
Kulik I O and Shekhter R I 1975 *Zh. Eksp. Teor. Fiz.* **68** 623 (Engl. transl. 1975 *Sov. Phys.–JETP* **41** 308)
Barner J B and Ruggiero S T 1987 *Phys. Rev. Lett.* **59** 807
Kuz'min L S and Likharev K K 1987 *Pis. Eksp. Teor. Fiz.* **45** 389 (Engl. transl. 1987 *JETP Lett.* **45** 495)
Early work reviewed by Likharev K K 1988 *IBM J. Res. Dev.* **32** 143
[13] Ekkens T B, Nolen S and Ruggiero S T 1996 *J. Appl. Phys.* **79** 7392
[14] Hanna A E and Tinkham M 1998 *Phys. Rev. Lett.* **80** 1956
[15] Amman M, Wilkins R, Ben-Jacob W, Parker P D and Jakelvic R C 1991 *Phys. Rev.* B **43** 1146
[16] Ruggiero S T and Barner J B 1991 *Z. Phys.* B **45** 333
[17] Schabowsa E and Szceklik J 1981 *Thin Solid Films* **75** 177
[18] Gray D E (ed) 1972 *American Institute of Physics Handbook* 3rd edn (New York: McGraw-Hill)
[19] Ozin G, Huber H, McIntosh D, Mitchell S, Norman J G Jr and Noodleman L 1979 *J. Am. Chem. Soc.* **101** 3504
[20] Ganz E, Sattler K and Clarke J 1988 *Phys. Rev. Lett.* **60** 1856
Ganz E, Sattler K and Clarke J 1989 *Surf. Sci.* **219** 33
[21] Sattler K 1986 *PDMS and Clusters, Proc. 1st Int. Conf. on the Physics of Small Systems (Wangerooge, 1986)* ed E R Hilf, F Kammer and K Wien (New York: Springer) pp 119–26
[22] Kittel C 1971 *Introduction to Solid-State Physics* (New York: Wiley) p 39
[23] Hansen L B, Stoltze P, Norskov J K, Clausen B S and Niemann W 1990 *Phys. Rev. Lett.* **64** 3155
[24] Andreoni W and Martins J L 1985 *Surf. Sci.* **156** 635